Journal of Statistical Physics, Vol. 58, Nos. 1/2, 1990

Gauge-Invariant Lattice Gas for the Microcanonical Ising Model

Richard C. Brower,[1] K. J. M. Moriarty,[2] Peter Orland,[3] and Pablo Tamayo[4]

Received May 8, 1989

We introduce a lattice gas for particles with discrete momenta $(1, 0, -1)$ and local deterministic microdynamics, which exactly reproduces Creutz's microcanonical algorithm for the ferromagnetic Ising model. However, because of the manifest gauge invariance of our variables, both the Ising ferromagnetic and spin-glass systems share precisely the same dynamics with different initial conditions. Additional conservation laws in the 1D Ising case result in a completely integrable system in the limit of zero or unbounded demon energy cutoff. Numerical investigations of ergodicity are presented for the pure Ising lattice gas in one and two dimensions.

KEY WORDS: Lattice gas; cellular automata; microcanonical ensemble; Ising model; deterministic dynamics; spin glass.

1. INTRODUCTION

Several years ago, Creutz proposed a deterministic microcanonical algorithm[1,2] as a particularly efficient way to run a Monte Carlo simulation of the Ising model. His formulation has led to very fast multispin codes for vector supercomputers that rival the best speeds for the standard heat bath algorithm on dedicated special processors.[3,4]

[1] Electrical, Computer and Systems Department, and Department of Physics, Boston University, Boston, Massachusetts.

[2] Institute for Computational Studies, Department of Mathematics, Statistics and Computing Science, Dalhousie University, Halifax, Nova Scotia, Canada, and Institute for Advanced Study and John von Neumann National Supercomputer Center, Princeton, New Jersey.

[3] Physics Department, Virginia Polytechnic Institute and State University, Blacksburg, Virginia.

[4] Physics Department and Center for Polymer Studies, Boston University, Boston, Massachusetts.

0022-4715/90/0100-0141$06.00/0

However, as pointed out by Bhanot *et al.*,[2] in such a purely deterministic scheme, ergodicity is harder to analyze. Although all Monte Carlo algorithms using pseudo random numbers are in fact deterministic, the class of algorithms which can be cast as a local dynamics on a finite set of bits clearly brings ergodicity more strongly into question. Indeed such algorithms, which are often referred to in the literature as cellular automata,[5] are known to exhibit a vast range of nonequilibrium phenomena from fluid flow[6] to continuous evolution as in the game of life.

All these questions become even more difficult and interesting for the Ising spin glass, which is known to have usual metastability properties and very slow relaxation rates in Monte Carlo dynamics.

Here we introduce a lattice gas on a hypercubic lattice with discrete momentum components $(1, 0, -1)$ on each axis and local scattering rules similar to the HPP lattice fluid investigated by Hardy *et al.*[7] For very specific initial conditions, these rules are equivalent to Creutz's deterministic microcanonical algorithm for the ferromagnetic Ising model. However, our dynamics is more general and studying it has led us to several interesting observations: (1) There is in fact a single lattice gas dynamics for both the Ising and the spin-glass systems, differing only in the initial conditions. (2) Special limiting cases of the 1D system are exactly integrable. (3) In two dimensions, the bath degrees of freedom diffuse at a rate nearly independent of the temperature.

We have also performed simulations of the length of individual orbits in the microcanonical phase space to investigate orbit distributions, averages, correlation functions, and ergodicity. One of our long-range goals is to arrive at a set of continuum dynamical equations, analogous to the time-dependent Ginzburg–Landau equations, which, however, encompass both ferromagnetic and spin-glass dynamics.

2. GAUGE-INVARIANT LATTICE GAS DYNAMICS

The local version of Creutz's microcanonical ferromagnetic Ising or spin-glass model consists of two sets of variables: first, the Ising spins $s_i = \pm 1$ for the magnetic moments at the sites on a periodic hypercubic lattice ($i_x = 1, 2, \ldots, L_x$; $i_y = 1, 2, \ldots, L_y$; etc.), with energy function

$$E_{\text{Ising}} = \sum_{\langle ij \rangle} (1 - J_{ij} s_i s_j) \tag{1}$$

and quenched nearest neighbor couplings, $J_{ij} = \pm 1$; second, the thermal bath variables, which are represented as uncoupled local variables $b_i = 0, 2, 4, \ldots, b_{\max}$ attached to each site with energy function

$$E_{\text{bath}} = 2 \sum_i b_i \tag{2}$$

The microcanonical dynamics changes the state variables keeping the total energy, $E_{\text{Tot}} = E_{\text{Ising}} + E_{\text{bath}}$, conserved.

To enforce time-reversal symmetry, Creutz defined a second-order dynamics so that two cycles in iteration time are required for a full update $t \to t+2$. At even/odd iteration cycles ($t =$ even/odd) the microcanonical dynamics attempts to flip each spin on all the red/black ($i_x + i_y + \cdots =$ even/odd) sites. The flip is accepted if and only if the local energy conservation at each sites does not force b_i to go out of range. With $b_{\max} = 0$ this update rule is equivalent to the $Q2R$ cellular automata rule of Bennett and Vichniac.[8]

2.1. Gauge-Invariant Equations of Motion

The microscopic equations of motion for gauge-invariant lattice gas (GILG) take the familiar form of a transport equation,

$$p_u(i+\mu, t+1) - p_\mu(i, t) = F_\mu(p_\mu(i, t), b(i, t)) \tag{3}$$

and a continuity (or energy conservation) equation,

$$b(i, t+1) - b(i, t) + \sum_\mu [p_\mu(i+\mu, t+1) - p_\mu(i, t)] = 0 \tag{4}$$

in terms of the bath varibles $b(i, t)$ and a new set of single bit variables $p_\mu(i, t)$,

$$e^{i\pi p_\mu(i,t)} = J_{i,j} s_i s_j \tag{5}$$

The dynamics is defined completely once the collision term F_μ is given, and it is obviously invariant under the local gauge transformations,

$$J_{i,j} \to \Omega_i J_{ij} \Omega_j, \qquad s_i \to \Omega_i s_i \tag{6}$$

where $\Omega_i = \pm 1$.

Our "momentum" variables $p_\mu(i, t)$ are defined on all directed links $j = i - \mu \to i$ with $\mu = \pm\hat{1}, \pm\hat{2}, \ldots, \hat{d}$. A link with an "on" bit $p_\mu(i) = 1$ is thought of as a "particle" or "ball" carrying momentum ± 1 corresponding to the Ising energy stored in that bond. With the positive momentum convention[5] we can write Eq. (3) as

$$2p_\mu(i, t) = 1 - J_{i,j} s_i s_j \tag{7}$$

The bath bits for $b(t, i)$ represent zero-momentum "particles" fixed at the lattice site i (Fig. 1).

[5] Note that negatively directed kinks carry momenta $-p_{-\mu}(i, t) = 0, -1$ and symmetry in i, j gives the identity $p_{-\mu}(i, t) = p_\mu(i-\mu, t)$, so that all p'_μ can be associated with either the red or black sites as one chooses.

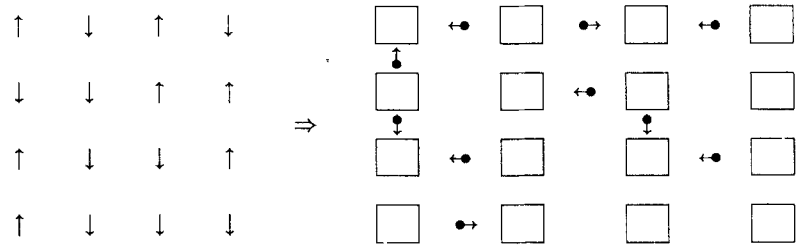

Fig. 1. Example of the mapping from a 2D Ising Ferromagnet to the gauge-invariant lattice-gas formulation. Balls represent the energy corresponding to links with $s_i s_j = -1$.

It is now easy to devise scattering rules that are equivalent to Creutz's cellular automaton. For convenience we begin by decomposing the dynamics in terms of *collisions* at the sites followed by *advection* to the next site. All sites i are divided into red and black pairs. At a given time t, the initial conditions are chosen so only the red or the black sites have balls colliding with it. The collision rules at those active sites can be written either as a Boolean expression,

$$p'_\mu(i, t) = p_{-\mu}(i, t) \otimes A(b(i, t), p_\mu(i, t)) \tag{8}$$

or as an arithmetic expression,

$$p'_\mu(i, t) = p_{-\mu}(i, t)[1 - A(b, p_\mu)] + [1 - p_{-\mu}(i, t)]\, A(b, p_\mu) \tag{9}$$

where $p_\mu = 1, 0$ corresponds to true and false respectively, and $\otimes$ is the "exclusive or." The acceptance function A is 1/0 (true/false) when the new demon energy is in bounds or out of bounds ($0 \leqslant b_i \leqslant b_{\max}$), respectively,

$$A(b, p_\mu) = \theta\left(b + \sum_\mu (2p_\mu - 1)\right) \theta\left(b_{\max} - b - \sum_\mu (2p_\mu - 1)\right) \tag{10}$$

Figure 2 shows collision rules for 2D in the form of scattering diagrams.[6] Now the advection of the moving balls, $p_\mu(i + \mu, t + 1) = p'_{-\mu}(i, t)$, and local energy conservation complete the derivation of the equations of motion (3), (4) with the collision term

$$F_\mu(b, p) = (1 - 2p_{-\mu})\, A(b, p) + (p_\mu - p_{-\mu}) \tag{11}$$

It is also interesting to consider a simpler rule closer to the HPP fluid microdynamics by dropping the constraint $p_{-\mu}(i, t) = p_\mu(i - \mu, t)$ and

[6] The rules can be easily extended to the case of bond dilution by prohibiting links with $J_{ij} = 0$ to transport a ball.

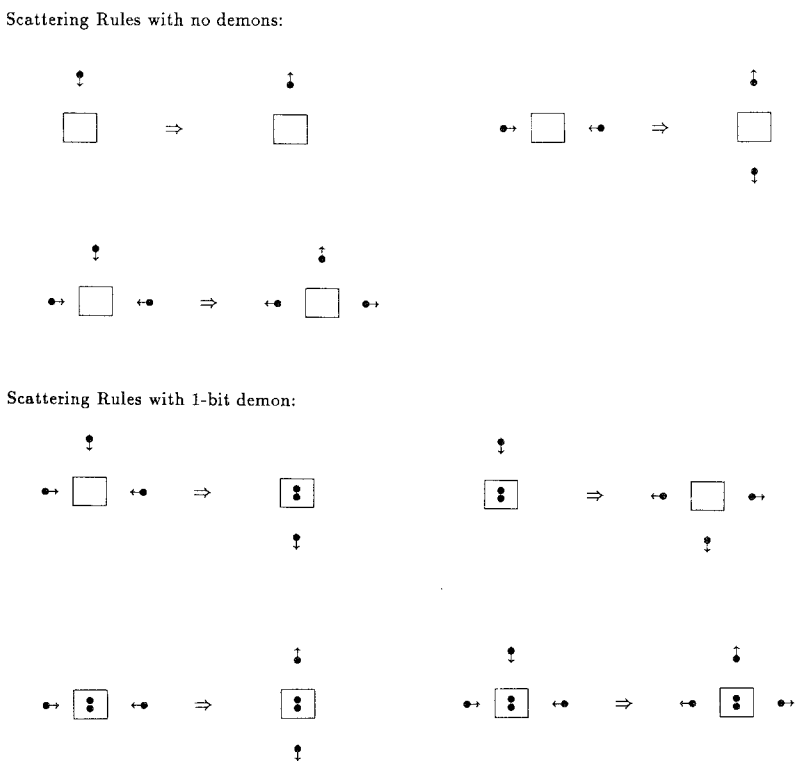

Fig. 2. Scattering rules for the energy balls. Moving balls, representing broken links, move toward red (black) sites during the red (black) phase of the update cycle. Stationary balls (always in pairs) represent bath or demon energy. While the total number of balls (moving plus stationary) is always conserved, momentum is not. Rules in which scattering does not occur are not shown.

allowing simultaneous red/black updates. This merely corresponds to two sets of independent Ising lattices (with spins $s_i^{(1)}$ and $s_i^{(2)}$) that share a common bath,

$$E_{\text{Tot}} = \sum_{\langle ij \rangle} (1 - J_{ij}^{(1)} s_i^{(1)} s_j^{(1)}) + \sum_{\langle ij \rangle} (1 - J_{ij}^{(2)} s_i^{(2)} s_j^{(2)}) + \sum_i 2b_i \qquad (12)$$

This uniform rule gives the same Ising equilibrium, and it probably has some advantages both as a parallel numerical algorithm and as a starting point for deriving the continuum dynamical equations. For the spin-glass case, the two spin replicas may help reduce critical slowing down.

3. GENERAL PROPERTIES OF THE LATTICE GAS DYNAMICS

In the remainder of this paper, we begin to explore the microdynamics of our gauge invariant lattice gas (GILG). Eventually we hope to take coarse-grain averages over blocks of sites to find an accurate effective field theory description analogous to the fluid equations of the HPP or FHP fluids[6] or a time-dependent Ginzburg–Landau equation for the pure Ising model.[9] However, such a theory must be quite subtle, since it should encompass both ferromagnetic and spin-glass behavior. We begin the program by identifying the conservation laws, pointing out a simple diffusion process in 2D, discussing the special integrability properties of 1D and reporting on some numerical simulations to support our contention that the 1D and 2D physics have quite different ergodicity properties.

2.1. Conservation Laws

While the above scattering rules are similar to the HPP lattice cellular automata fluid, we have a very different set of conservation laws. The gauge-invariant lattice gas dynamics does conserve particle number (or energy), but momentum is not conserved except in 1D (see Section 4 for a discussion of the special properties of 1D dynamics).[7] Presumably in 2D and higher for the ferromagnetic Ising case, the macroscopic equations are of the diffusive transport type, which in turn imply the model C dynamics of Hohenberg and Halperin,[9] but there is no analogue of the Navier–Stokes equations. As we note below, numerical simulations indicate a simple underlying diffusion mechanism for the bath particles. We are also doing simulations to measure the autocorrelation functions and see if the critical dynamics is in fact model C.[10,11]

The reason that the spin-glass dynamics is subsumed in this rule is tied to the existence of an infinite number of local conservation rules (one for each plaquette),

$$Q_{\mu\nu}(i, t) = (p_\mu(i, t) + p_\nu(i+\mu, t) - p_\mu(i+\nu, t) - p_\nu(i, t)) \bmod 2 \quad (13)$$

which are a consequence of the gauge symmetry mentioned above in Eq. (3). Thus, the scattering rules must conserve mod 2 the total number of balls on the edges of a plaquette. If all plaquettes have even numbers of balls, there are no frustrated plaquettes, but an odd number of balls means that the plaquette is permanently frustrated. Since this frustration "parity" is a property of the initial distribution of balls, the dynamics of a

[7] If we consider the case $b_{\max} = 0$, our scattering rules differ from the HPP rule only for the cases involving an odd number of balls, which alone violate momentum conservation.

spin glass is exactly the same as a local Creutz microcanonical rule for the unfrustrated Ising model, up to initial conditions. Again this has similarities and dissimilarities with the cellular automata fluids.[6] For the CA fluid, we know that there are two types of initial conditions that lead to laminar or turbulent dynamics, respectively. Because of the exact symmetries of the discrete lattice fluid, a perfectly uniform flow will always stay laminar. The complexity of the subsequent dynamics that distinguishes between laminar or turbulent is coded in the initial conditions analogous to the choice between ferromagnetic or spin-glass dynamics for the Ising lattice gas. However, there are major differences. In the Ising lattice gas, the frustration (unlike vorticity) stays fixed in number and location, whereas for the HPP fluid, vorticity can be created as one moves along an orbit.

One dimension is very special, as we discuss below. In 1D there are just as many $p_\mu(i)$ bond variables as s_i spin variables, so that gauge invariance is a trivial redefinition of the spins. Also, momentum is conserved. More surprisingly, the numbers of positive and negative momentum components are essentially separately conserved at low density. It is likely that the continuum equations of one dimension bare little resemblance to the ones at higher dimensions.

3.2. Continuum Diffusion of Bath Particles

It is interesting to try to understand the dynamics for coarse-grain-average quantities such as the energy densities,

$$\rho_{\text{bath}}(x, t) = \langle b(i, t) \rangle, \qquad \rho_{\text{Ising}}(x, t) = \sum_{\mu > 0} \langle p_\mu(i, t) + p_{-\mu}(i, t) \rangle \quad (14)$$

where the notation $\langle \cdots \rangle$ indicates an average over a large block of sites centered at x and the sum extends over all the positive directions $\mu = \hat{1}, \hat{2}, \ldots, \hat{d}$. For example, the linear continuity equation (4) might be approximated by expanding the finite differences to first order to get

$$\partial_t \rho_{\text{bath}} + \partial_t \rho_{\text{Ising}} + \nabla \cdot (\rho_{\text{Ising}} \mathbf{V}) = 0 \quad (15)$$

in terms of the mean velocity V_μ defined by

$$\rho_{\text{Ising}} V_\mu(x, t) = \frac{\Delta x}{\Delta t} \langle p_\mu(i, t) - p_{-\mu}(i, t) \rangle \quad (16)$$

However, when one considers the nonlinear collision term in the transport equation (3) and the gauge constraints (13), reliable approximations are far from obvious. If continuum approximations are possible at all for

the spin-glass, one will have to allow for some kind of topological singularities to represent frustrated plaquettes. One test of the resulting continuum equations of motion is to demand that they be equivalent to the time-dependent Ginzburg–Landau equations for the average spin field $\phi(x, t) = \langle s_i(t) \rangle$ in the limit of zero frustrations.

Numerical simulations can also offer a guide. For example, it is interesting to notice that the temperature-dependent diffusion "constant" for the equilibration of the effective thermal field $T(x, t) = 1/\beta(x, t)$, derived by Creutz[12] in 2D, in fact corresponds to a fixed diffusion constant for the density of the bath particles $\rho_{\text{bath}}(x, t)$.

Creutz simulated the microcanonical Ising model with a thermal gradient, and by measuring the heat flow,

$$\mathbf{Q} = -\kappa \nabla T \tag{17}$$

found that the thermal conductivity depended strongly on temperature ($\kappa \simeq 24\beta^2$). To convert this result to the conduction of demons ($\mathbf{Q} = -D\nabla\rho_{\text{bath}}$), we expand ρ_{bath} at high temperaure, assuming local thermal equilibrium,

$$\rho_{\text{bath}}(x, t) = 3 - 10\beta(x, t) + \cdots \tag{18}$$

As a result the new diffusion coefficient for the ρ_{bath} field is a nearly fixed constant ($D \simeq 2.4$) in the region above the phase transition. Hence the demon balls undergo Brownian motion, with its density ρ_{bath} governed by an almost linear diffusion equation. Presumably as one approaches the phase transition nonlinearities develop similar to those found by Boghosian and Levermore in their deterministic cellular automata diffusion model.[13]

4. INTEGRABILITY IN ONE DIMENSION

Equilibrium is not always attained by classical systems with many degrees of freedom over long time scales. This was first noticed by Fermi *et al.*,[14] who simulated a 1D system of weakly coupled harmonic oscillators on the MANIAC I at Los Alamos. Specifically, they found no tendency to equipartition among the normal modes. Further investigations of this system were made by Ford and Waters[15] and Zabusky and Kruskal,[16] who recognized that the failure of equipartition was due to the fact that soliton modes were present, and that scattered solitons maintained their integrity; the system is, in fact, a lattice version of the Korteweg–DeVries equation. The work of Toda and of Flaschka[17] finally led to a complete understanding of the inverse scattering transform.

One dimension is very special. In 1D the total momentum is actually conserved. Also, there are just as many $p_\mu(i)$ bond variables as s_i spin variables, so that gauge invariance is a trivial redefinition of the spins. Moreover, the ± 1 momentum particles are equivalent to right- and left-moving kinks, respectively.

Now we will show that if b_i is unbounded, $b_{\max} = \infty$, the system is always integrable. Consider a configuration with $b_i = 0$, for all i. Furthermore, at $t = 0$ and j odd in some large neighborhood take $s_i = 1$, $i \leqslant j$, and $s_i = -1$, $i > j$. This configuration is a right-moving particle ($p_{\hat{1}} = 1$) or kink. With periodic boundary conditions the total number of kinks is even, so an antikink must exist somewhere else. In our lattice gas description at $t = 0$ right (or left-) moving kinks are represented by a ball moving on a link with $p_{\hat{1}}(i, t) = 1$ [or $p_{-\hat{1}}(i, t) = 1$] for $i =$ even (odd). As we apply Creutz's dynamics, the balls (kinks) move with constant velocity to the right or left.

Left- and right-moving kinks can scatter. Again, take $b_i = 0$ everywhere and suppose there is one left-moving and one right-moving kink. When the kinks reach the same site k, there is an energetic loss in E_{Ising} which is made up for by a transition from $b_j = 0$ to $b_j = 2$ or increasing E_{bath}. This excitation at the site k (two balls bound together) remains for two time steps before decaying into a pair of balls (kinks) again. The scattering can be represented symbolically as in Fig. 3. The balls may be thought of as real particles which, upon colliding, stick together, before

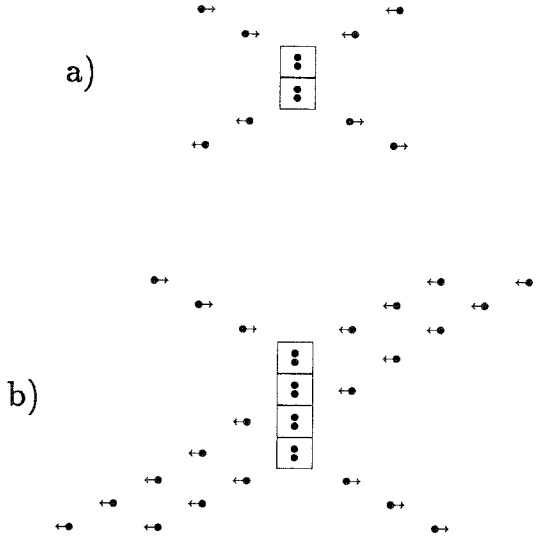

Fig. 3. Examples of scattering events in 1D: (a) Two-body scattering. (b) Three-body scattering.

reversing direction. The phase shift, or bound-state lifetime, is always the same.

If $b_i > 0$ at some site, then b_i can be thought of as the number of bound states of two kinks. For example, if we take a configuration with no kinks and $b_i = 0$ everywhere except for $i = j$, then (for large N) b_j will emit pairs of kinks at discrete intervals until $b_j = 0$. With With $b_{\max} = \infty$, there is no restriction on the number of balls in a bound state at a single site.

Any configuration of the system has a unique representation in terms of kinks and kink-bound states. In this representation, it is easy to see why the system is integrable. It is because, in N-body scattering, the phase shifts are *additive*. There is no connected many-body scattering term. Consider the case of three-body scattering in Fig. 3. First two kinks form a bound state. The bound state does not have the opportunity to decay before it is intercepted by another kink. However, each kink is phase-shifted by exactly twice the number of kinks moving in the opposite direction. Thus, any scattering of any number of kinks can be thought of as a sequence of two-body scatterings.

Even if $b_{\max} < \infty$, the system will be integrable if the phase space is appropriately restricted. For example, if $N \leqslant b_{\max} < \infty$ the system will act as if $b_{\max} = \infty$. It is also trivial to extend our argument to the case of $b_{\max} = 0$, where there is no scattering at all. For intermediate values of $b_{\max}$ there are scattering events which form bound states up to $b_{\max}$ balls, but if another simultaneous collision occurs that collision is elastic. Hence, there is a critical density where the system crosses over from one case to the other. Integrability is not obvious in this situation.

4. NUMERICAL RESULTS AND RECOMMENDATIONS

We first noticed the integrability of the 1D system in a computer simulation of the lattice gas dynamics. This caused us to seriously question ergodicity in this lattice gas dynamics. In one dimension, independent of $b_{\max}$, there is an additional momentum conservation law that fixes the number of right-moving minus left-moving kinks (balls), so the single orbit may cover only a small portion of the energy surface. Indeed, on a finite lattice at low kink density our argument implies that a typical orbit will have length $T_{\text{orbit}} = O(N)$. This is clearly not true ergodic behavior.

To check for this nonergodic behavior we have simulated the 1D system for a range of values of N and measured the length (T_{orbit}) of the orbits encountered. To select a "typical" orbit on the energy surface in 1D and 2D, we pick a random starting configuration of the Ising and bath variables in thermal equilibrium. This allows us to find orbits on the energy sphere with a probability given approximately by the relative size of the

orbit. Our procedure is as follows. We first simulate the canonical Ising system,

$$\text{Prob}\{s_i\} = (1/Z)\exp\left[-\beta \sum_{\langle ij\rangle} (1 - s_i s_j)\right] \tag{19}$$

via heat bath to get an initial value of the spins (or moving balls). Then we obtain the analytical expression for the mean total energy for the system in equilibrium at temperature β,

$$E_{\text{Tot}}(\beta) = \langle E_{\text{Ising}} \rangle + \langle E_{\text{bath}} \rangle \tag{20}$$

from the mean bath energy,

$$\langle E_{\text{bath}} \rangle = N \sum_{b=0}^{b_{\max}} 2b \exp(-2\beta b) \Big/ \sum_{b=0}^{b_{\max}} \exp(-2\beta b) \tag{21}$$

and from the mean Ising energy,

$$\langle E_{\text{Ising}} \rangle = -J(N-1)\tanh(\beta J) \tag{22}$$

in 1D or the corresponding Onsager solution on a finite torus[18] in 2D. From these expressions and the instantaneous value of the Ising energy, we calculate the deficit in the total energy at fixed β to find the bath energy. The requisite number of bound-state bath balls is then set by choosing their initial position at random. Under the assumption of equilibrium this algorithm chooses orbits at random on a fixed-energy sphere with probability weighted roughly by their length (T_{orbit}). In Fig. 4 we plot the cumulative distribution function (CDF)

$$F(T_{\text{orbit}}) = \int_0^{T_{\text{orbit}}} \rho_{\text{orbit}}(T)\, dT \tag{23}$$

as a function of T_{orbit} and system size N for 1D. The failure of ergodicity[2] is signaled by the slow growth in the largest orbits as $N \to \infty$ relative to the exponential growth of the energy sphere or entropy of the system. In Fig. 5 the orbit CDF is plotted against $\log(T_{\text{orbit}})/N$.

We have repeated this same procedure for picking the orbits in the 2D Ising lattice gas. The numerical results exhibit several interesting features (see Fig. 6). First, for very small systems, there are many small orbits, but as N exceeds about 10×10, the large orbits dominate and rapidly become so dominant that above $N = 32 \times 32$ we were unable to find any orbit under 50,000. As expected for ergodic behavior the orbit CDF scales approximately as a function of $\log(T_{\text{orbit}})/N$. In fact, as anticipated by

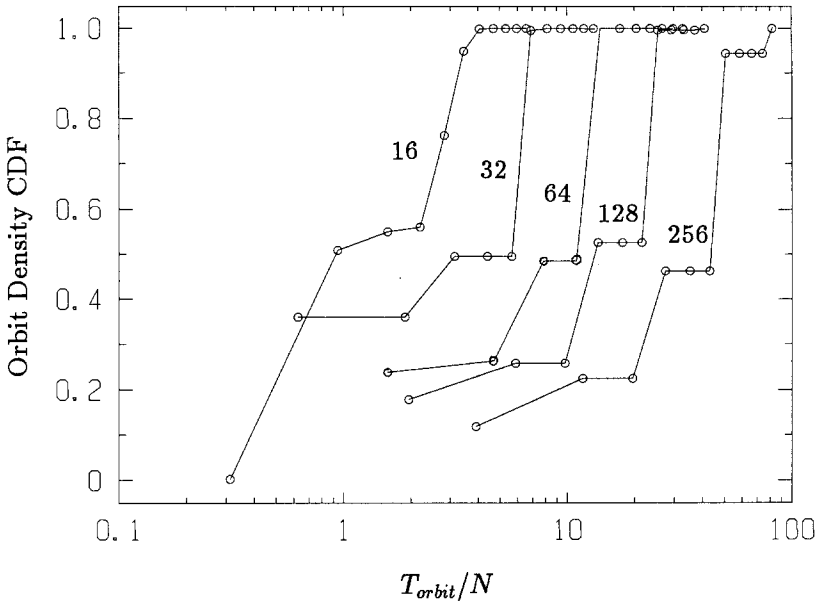

Fig. 4. Orbit cumulative distribution function vs. T_{orbit}/N, for 1D systems.

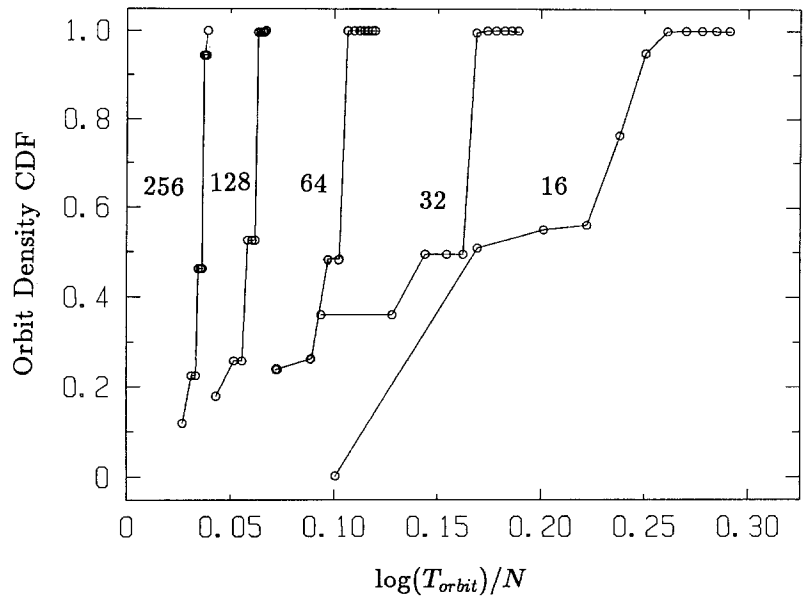

Fig. 5. Orbit cumulative distribution function vs. $\log(T_{\text{orbit}})/N$, for 1D systems.

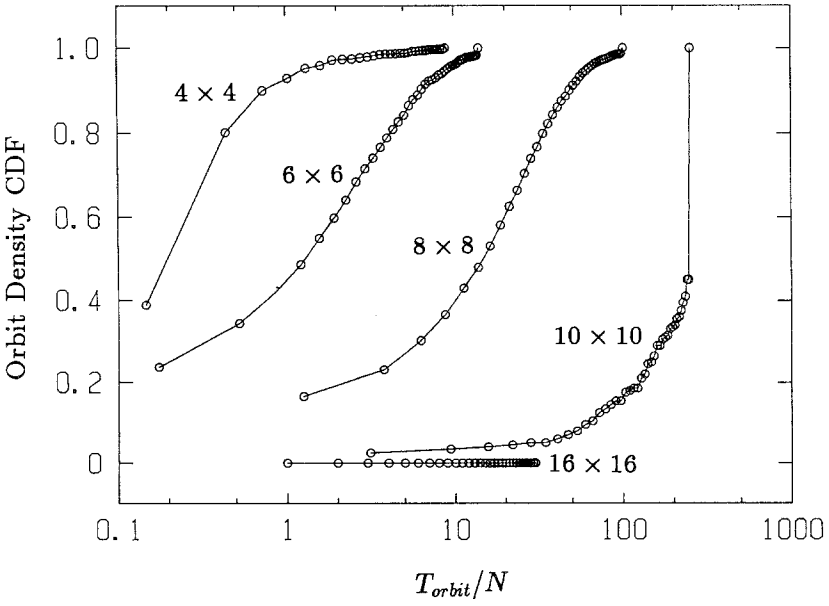

Fig. 6. Orbit cumulative distribution function vs. T_{orbit}/N, for 2D systems.

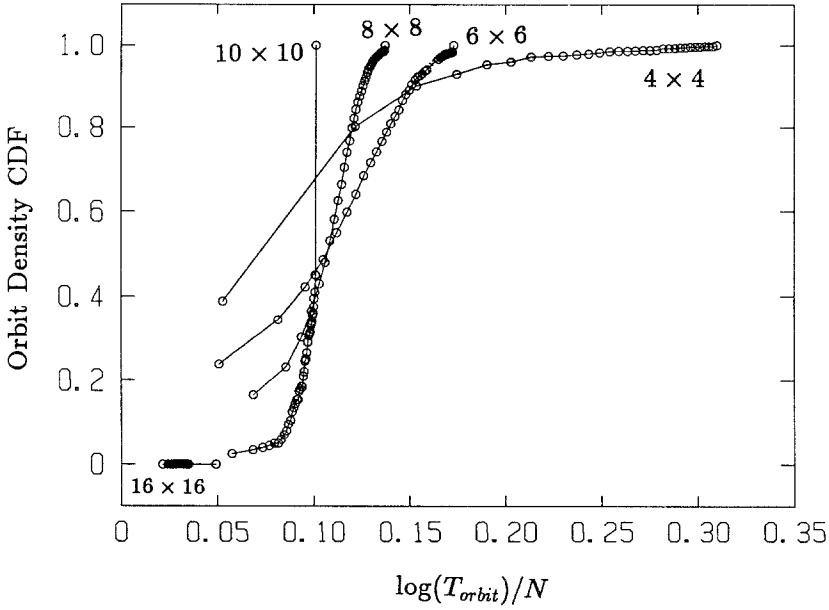

Fig. 7. Orbit cumulative distribution function vs. $\log(T_{\text{orbit}})/N$, for 2D systems.

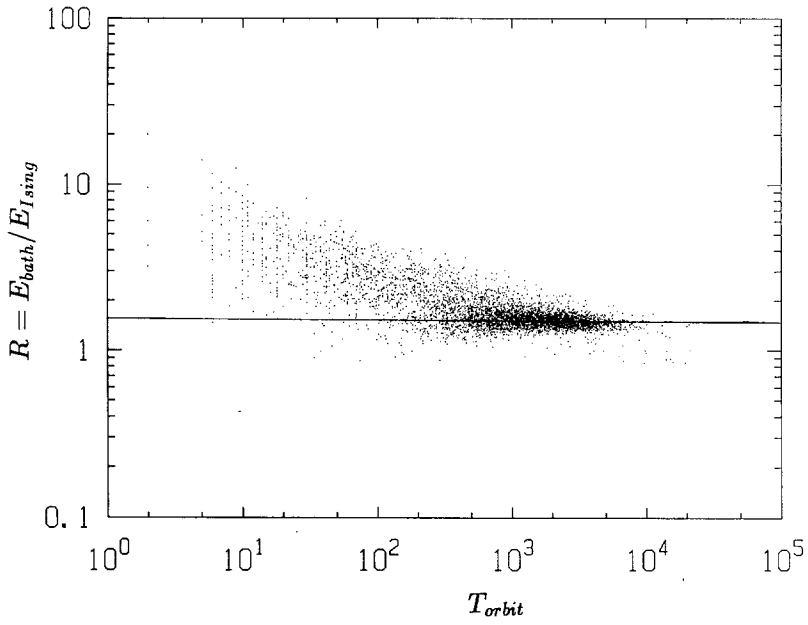

Fig. 8. Ratio $R = E_{\text{bath}}/E_{\text{Ising}}$ for a set of orbits in a 2D 8×8 system. The solid line indicates the value of R for the corresponding canonical ensemble in thermal equilibrium.

Bhanot *et al.*[2] the limiting profile is consistent with the ergodicity requirement that one giant orbit consumes all but a small, finite part of the energy sphere. This feature can be seen more easily in Fig. 7, in which the orbit CDF is plotted against $\log(T_{\text{orbit}})/N$. Obviously, our data are only suggestive. These are very difficult inferences to draw from simulations, but the contrast between the 1D and 2D dynamics is evident.

Then, as a second check on ergodicity, we compare time averages for the partition between the Ising and bath energy $R = E_{\text{bath}}/E_{\text{Ising}}$ on individual orbits as a function of the size of the orbit (T_{orbit}) and the size of the system (N). Hence we are able to compare the exact microcanonical partition of energy (on an entire orbit) with the exact result for the canonical distribution in thermal equilibrium (see equation above). In Fig. 8, we see the comparison for a random selection of orbits in a 8×8 system; the solid line indicates the value of R for the canonical distribution. With our algorithm for choosing orbits, we can show that the mean values over orbits should converge to the mean value of the canonical ensemble independent of the lack of ergodicity of individual orbits.

5. CONCLUDING REMARKS

In conclusion, we see that on both theoretical and numerical grounds ergodicity is compromised in the 1D local microcanonical Ising dynamics. On the other hand, the numerical analysis of the distribution of orbits in the 2D dynamics does not indicate the same difficulty with ergodicity except for very small lattices.

The insight that the lattice gas approach affords warrants in our opinion further theoretical and numerical investigation. In purely practical terms, if computer codes based on the lattice gas dynamics are to challenge traditional Metropolis methods, two conditions must be met: (1) They

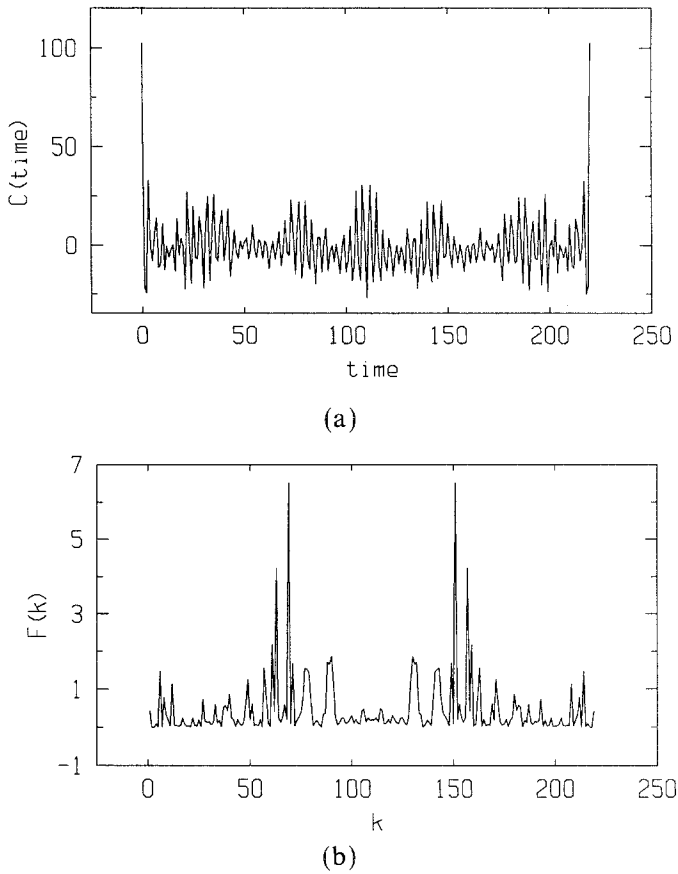

Fig. 9. Example of (a) connected part of the energy autocorrelation function and (b) its corresponding Fourier transform for a 2D 8×8 system. It shows peculiar periodicities and negative correlations. It does not exhibit exponential behavior.

must exhibit ergodicity, so that time averages of the dynamics are equivalent to thermal averages. (2) They must not exhibit longer relaxation times or worse critical slowing down to the point where this overwhelms their algorithmic speed advantage.

At present we are measuring the autocorrelations in the 2D Ising model to determine the dynamical critical exponent for critical slowing down. As we see in Fig. 9, in small lattices on individual orbits the autocorrelations do not exhibit exponential behavior. Consequently, it is difficult to use finite-size effects in small lattices to measure autocorrelations, and at the very least we must average over autocorrelations in a large ensemble of orbits. Results on the critical slowing down of both local and nonlocal microcanonical Creutz dynamics will be reported in a subsequent publication.

Also, by understanding the various versions of this local lattice gas dynamics, one has an efficient tool for studying nonequilibrium physics, such as domain formation, growth, and even fluid motion. In these applications one needs to establish the relationship between iteration time and real time, and if possible to find the macroscopic equations of motion for average quantities to better understand the physical consequences.

An even more interesting problem is to study the dynamics of the gauge-invariant lattice gas (GILG) in the presence of frustrations. It will be interesting to compare the orbit size distribution for ferromagnetic versus spin-glass initial conditions in higher dimensions. The ultrametric structure of the spin glass and the long-lived metastable states should be reflected in this phase space portrait, if the lattice gas is a faithful reflection of the canonical ensemble distribution.

How this correspondence comes about (if it does) is not trivial and we anticipate that much longer simulations will have to be performed before a clear picture emerges.

ACKNOWLEDGMENTS

We thank Mike Creutz and Roscoe Giles for useful discussions. We thank Tom Toffoli for bringing to our attention another discussion of the advantage of bond energy variables[19] in microcanonical Ising dynamics. We also thank Joao Leao of the Physics Computer Center at Boston University, Lloyd M. Thorndyke and Carl S. Ledbetter of ETA Systems, Inc., and Robert M. Price, Lawrence Perlman, and Gill Williams of Control Data Corporation for their continued interest, support, and encouragement, and access to the Scientific Information Services CDC CYBER 205 at Kansas City, Missouri. We thank the National Allocation Committee for the John von Neumann National Supercomputer Center for access to

the two CDC CYBER 205's at JvNC (grants 110128, 551702, and 551705); the Control Data Corporation PACER Fellowship grants (grants 85PCR06, 86PCR01, and 88PCR01) for financial support; ETA Systems, Inc., for financial support (grants 304658, 1312963, and 1333824); the National Sciences and Engineering Research Council of Canada (grants NSERC A8420 and NSERC A9030) for financial support; the Continuing Education Division, Technical University of Nova Scotia, for financial support; and the Canada/Nova Scotia Technology Transfer and Industrial Innovation Agreement (grants 87TTII01 and 88TTII01) for further financial support.

REFERENCES

1. M. Creutz, *Phys. Rev. Lett.* **50**:1411 (1983).
2. G. Bhanot, M. Creutz, and H. Neuberger, *Nucl. Phys. B* **235**:417 (1984).
3. H. Herrmann, Saclay Preprint 86-060 (1986).
4. M. Creutz and K. J. M. Moriarty, *Comp. Phys. Comm.* **39**:173 (1986).
5. Proceedings, Workshop on Cellular Automata, *Physica D* **10D** (1984).
6. N. Margolus, T. Toffoli, and G. Y. Vichniac, *Phys. Rev. Lett.* **56**:1696 (1986); U. Frish, B. Hasslacher, and Y. Pomeau, *Phys. Rev. Lett.* **56**:1505 (1986); D. D'Humieres, P. Lallemand, and T. Shimonura, Los Alamos National Laboratory Preprint LA-UR-85-4051 (1985); S. Wolfram, Cellular Automata Fluids 1: Basic Theory, Technical Report CA86-2, Thinking Machines Corp. (1986).
7. J. Hardy, O. de Pazzis, and Yves Pomeau, *Phys. Rev. A* **13**:1949 (1976).
8. G. Y. Vichniac, *Physica* **10D**:96 (1984).
9. P. C. Hohenberg and B. I. Halperin, *Rev. Mod. Phys.* **49**:435 (1977).
10. R. C. Brower, K. J. M. Moriarty, Eric Myers, P. Orland, and P. Tamayo, *Phys. Rev. B* **38**:11471 (1988).
11. R. C. Brower and P. Tamayo, in preparation.
12. M. Creutz, *Ann. Phys.* **167**:62 (1986).
13. B. Boghosian and C. D. Levermore, A cellular automaton for Burgers' equation, *Complex Systems* **1**:17 (1987); A deterministic cellular automaton with diffusive behavior, unpublished.
14. S. Ulam, E. Fermi, and J. Pasta, Los Alamos Sci. Lab. Rept. LA-1940 (1955).
15. J. Ford, *J. Math. Phys.* **2**:387 (1961); J. Ford and J. Waters, *J. Math. Phys.* **4**:1293 (1963).
16. N. J. Zabusky and M. D. Kruskal, *Phys. Rev. Lett.* **15**:240 (1965).
17. M. Toda, *Prog. Theor. Phys. Suppl.* **59**:1 (1976); H. Flaschka, *Prog. Theor. Phys.* **51**:703 (1974).
18. A. E. Ferdinand and M. E. Fisher, *Phys. Rev.* **185**:832 (1969).
19. C. H. Bennett, N. Margolus, and T. Toffoli, *Phys. Rev. B* **37**:2254 (1988).